JOURNAL OF SOLID STATE CHEMISTRY 111, 178–189 (1994)

The Composition Dependence of the Structure of Potassium-Loaded Zeolite A: Evolution of a Potassium Superlattice

A. R. Armstrong

ISIS Science Division, Rutherford Appleton Laboratory, Chilton, Didcot, Oxon OX11 0QX, United Kingdom

and

P. A. Anderson and P. P. Edwards[1]

The School of Chemistry, University of Birmingham, Edgbaston, Birmingham B15 2TT, United Kingdom

Received November 23, 1993; in revised form March 8, 1994

IN HONOR OF C. N. R. RAO ON HIS 60TH BIRTHDAY

Three samples of potassium zeolite A, containing 1, 3, and 5 additional potassium atoms per primitive unit cell, were prepared through the controlled reaction of dehydrated potassium zeolite A with a calibrated amount of potassium vapor. The structures of these materials, and that of the host dehydrated K_{12}-A, were determined by Rietveld refinement of powder neutron diffraction data. The structures of K_{12}-A and the most lightly loaded sample *with one extra potassium atom per unit cell* (K_1/K_{12}-A) were refined in space group $Pm\bar{3}m$ assuming disorder of Si and Al. For the more heavily loaded samples K_3/K_{12}-A and K_5/K_{12}-A a superlattice was observed, resulting in a doubling of the unit cell in space group $Fm\bar{3}m$. This superlattice arises as a result of potassium ordering. On potassium inclusion additional potassium sites K3 in the sodalite cage and K4 in the α cage are observed. At low loadings occupation of the site in the sodalite cages begins. The separation between the first of these two sites and K1 on the *opposite of the 6-ring windows is such that the two sites cannot be* occupied simultaneously, leading to occupation of the second new site facing the 4-rings of the α cage. The occupancies of these two new sites increase with increasing loading levels until ordering occurs. At limiting loading a tetrahedron of K3 forms in each sodalite cage, with alternate α cages containing 8 K1 and 12 K4, respectively. The possible role of K_4^{3+} in directing the formation of the superlattice is discussed.

INTRODUCTION

As a result of their regular intracrystalline cavities, zeolites have long been valued as "molecular sieves" and catalysts. More recently, interest has grown in the idea of using these minerals and their synthetic analogues as host materials for the creation of new solid state compounds (1–3). To date most attention has focused on the "guest" components, whose desirable properties are, one hopes, enhanced through encapsulation within the aluminosilicate host, the latter generally being accorded the role of passive matrix, moderating interactions between guest species through the imposition of a set geometrical arrangement. An important counterbalance to this prevailing view may be found in the study of alkali-metal-loaded zeolites, where the interaction between guest metal atoms and the zeolite host itself is so strong that spontaneous ionization of the former is observed, leading to the formation of a wide range of entirely new inclusion compounds, whose properties are inadequately expressed in terms of those of the parent alkali metal. Such compounds were first reported by Rabo *et al.* in 1966 (4), who observed a bright red color on exposing sodium zeolite Y to sodium vapor under vacuum. This was attributed to the formation of Na_4^{3+} centers, which had previously been observed on irradiation of the same zeolite (5). The reaction of sodium zeolite X with sodium vapor was found to impart a blue color, which was interpreted as arising from Na_6^{5+} centers. Subsequently the existence of K_4^{3+} (6, 7), K_3^{2+} (8), Na_5^{4+} (9), and Na_3^{2+} (10) *has been confirmed in zeolites X, Y, and A. The fact that* these paramagnetic centers have only been observed in zeolites whose structure contains sodalite cages strongly suggests that they reside within these structural units.

The electronic and magnetic properties of these compounds have been extensively studied through electron spin resonance (ESR), and in a few cases other spectroscopic techniques including solid state nuclear magnetic resonance (11, 12). The tetrahedral geometry of Na_4^{3+} was established by Rao and co-workers through Raman spectroscopy (13). The characteristic ESR spectra of the paramagnetic centers mentioned above are observed only

[1] To whom all correspondence should be addressed.

0022-4596/94 $6.00

at low concentrations of added metal. At higher concentrations dark solids are produced with single-line ESR spectra which have widely been attributed to the formation of metallic clusters within the zeolite pores. More recent work has cast doubt on this interpretation and suggests that coupling between adjacent centers leads to loss of the ESR hyperfine structure, resulting in a featureless singlet (11). The possibility of delocalization of electrons throughout the zeolite structure is of particular interest (11, 14), as in some ways dehydrated zeolites serve as experimental counterparts to free electron theories of metallic behavior. Thus the cations of dehydrated potassium zeolite A, for example, represent a more or less regular array into which precise numbers of electrons may be injected through reaction with controlled amounts of potassium vapor.

While a large number of spectroscopic studies have been performed on these materials, there have been very few structural investigations. We have studied the inclusion compounds of several potassium zeolites (15, 16), while Seff and co-workers have studied a number of compounds by single crystal X-ray diffraction, including those of K, Rb, and Cs zeolite A (17–21). The latter were prepared by reacting a single crystal of dehydrated Na_{12}-A with flowing alkali vapor in a combined ion exchange/inclusion reaction. A significant drawback of this technique is that control over product stoichiometry is limited, unlike the method outlined below.

EXPERIMENTAL

The compounds K_1/K_{12}-A, K_3/K_{12}-A, and K_5/K_{12}-A were prepared through the reaction of dehydrated potassium LTA (K_{12}-A) with controlled amounts of potassium vapor, equivalent to 1, 3, and 5 potassium atoms per primitive unit cell, respectively. The reactions were carried out at temperatures between 200 and 250°C in sealed, evacuated quartz reaction tubes, as described previously (11). The zeolite used was prepared from the sodium form (purchased from BDH) by standard ion exchange (22); near complete exchange was confirmed by atomic absorption and the crystallinity of the resultant material was checked by powder X-ray diffraction. A suitable amount of zeolite (typically 1–2 g) was placed in a reaction tube heated gradually to 450°C and evacuated overnight to better than 10^{-5} mbar.

The reaction tube was then taken into a high-quality argon glovebox where high-purity potassium metal (Aldrich, 99.95%), previously distilled into calibrated capillary tubes (11), was introduced, and returned to the vacuum line to be evacuated and sealed with a gas torch. At no stage did the metal come into contact with the atmosphere. When the sealed tube was later heated, the alkali metal vapor filled the reaction chamber and spontaneous coloration of the zeolite occurred. Careful annealing resulted in intense blue (K_1/K_{12}-A), dark brown (K_3/K_{12}-A), and greenish brown (K_5/K_{12}-A) solids. In the case of K_5/K_{12}-A a small amount of unreacted potassium formed a mirror on the surface of the quartz tube, indicating that a limiting composition had been reached.

A portion of each sample was sealed in the Spectrosil section of the reaction tube so that ESR measurements could be made without exposing the product to air. The spectra were recorded on a Varian E-109 spectrometer operating at X-band frequencies (9.3 GHz) with 100 kHz field modulation. The microwave frequency was measured with a Hewlett–Packard 5342A frequency counter to an accuracy of ±1 kHz, and g values were determined through comparison of the resonant field with that of the 1,1-diphenyl-2-picrylhydrazyl radical (DPPH).

Neutron powder diffraction measurements were performed on the POLARIS high-intensity, medium-resolution diffractometer at the ISIS pulsed source at the Rutherford Appleton Laboratory. Data were collected at room temperature for all the samples (including the dehydrated host zeolite K_{12}-A) and also at 4 K for K_1/K_{12}-A. Since the alkali-loaded zeolites are highly air sensitive, the room temperature data were collected with the samples still in their quartz reaction vessels. In order to eliminate the amorphous silica background, data were also obtained from an empty sample tube. These data were then smoothed, appropriately scaled, and subtracted from the zeolite diffraction patterns to produce an essentially flat background. For the low-temperature study of K_1/K_{12}-A the sample was transferred, in a high-quality argon glovebox, to a vanadium can fitted with an indium seal. On removal from the glovebox the sample can was rapidly inserted in the cryostat. The integrity of the sample was confirmed after the experiment as the characteristic blue color remained intact.

The structures were refined by the Rietveld method using the program TF14LS based on the Cambridge Crystallographic Subroutine Library (23, 24). Neutron scattering lengths of 0.367, 0.41534, 0.3449, and 0.5803 (all $\times$ 10^{-12} cm) were assigned to K, Si, Al, and O, respectively (25). The initial model for all the structure refinements used the primitive space group $Pm\bar{3}m$ (12Å cell), which assumes disorder of silicon and aluminium, and included all framework atoms and the principal potassium sites K1 at (x, x, x) $(x \sim 0.23)$ and K2 at $(0, x, x)$ $(x \sim 0.5)$. The space group $Fm\bar{3}c$ (24Å cell), in which silicon and aluminium are ordered, was also used in a number of cases. Since there were no reflections of significant intensity arising from the larger cell, and the reduction in symmetry was found to have no influence upon the position or occupancy of the potassium sites (the main reason for this study), $Pm\bar{3}m$ was adopted for all later refinements. In the first instance isotropic temperature factors were assigned to all atoms; however, the use of anisotropic thermal parameters for the host dehydrated zeolite A was

found to yield a marked improvement in the fit. As a result anisotropic temperature factors were used in all succeeding refinements, except for minor potassium sites. Potassium sites in addition to K1 and K2 were located using observed and difference Fourier methods with subsequent refinement and by testing minor sites reported in previous structural studies of zeolite A.

RESULTS AND DISCUSSION

a. K_{12}-A and K_1/K_{12}-A

The refinement of the structure of K_{12}-A in space group $Pm\bar{3}m$, using the starting coordinates of Pluth and Smith (26), converged rapidly to give the final parameters shown in Tables 1a and 1b. Sites K1 and K2 proved to be the only significant potassium positions observed in K_{12}-A, in broad agreement with previous studies of this material (26, 27). This results in a total potassium content of less than 12, as implied by studies which have reported a Si to Al ratio of greater than unity (26). The fit to the data is shown in Fig. 1a.

For the potassium-loaded material K_1/K_{12}-A there was a slight expansion in lattice constant from 12.2962(4) to 12.3061(1) Å. Observed and difference Fourier methods indicated the presence of an additional potassium site (K3) within the sodalite cage at around (0.12, 0.12, 0.12).

TABLE 1a
Structural Parameters for K_{12}-A and K_1/K_{12}-A in Space Group $Pm\bar{3}m$

	K_{12}-A (295 K)	K_1/K_{12}-A (295 K)	K_1/K_{12}-A (4 K)
Cell constant (Å)	12.2962 (4)	12.3061 (1)	12.2952 (1)
Si/Al			
x	0	0	0
y	0.1855 (3)	0.1852 (3)	0.1848 (4)
z	0.3782 (2)	0.3771 (2)	0.3791 (3)
O1			
x	0	0	0
y	0.2445 (3)	0.2417 (3)	0.2475 (3)
z	0.5	0.5	0.5
O2			
x	0	0	0
$y = z$	0.2855 (2)	0.2889 (1)	0.2827 (1)
O3			
$x = y$	0.1114 (2)	0.1123 (2)	0.1124 (2)
z	0.3585 (2)	0.3538 (2)	0.3603 (2)
K1			
$x = y = z$	0.2271 (5)	0.2343 (5)	0.2268 (4)
Site occupancy	1	0.82 (2)	0.76 (1)
K2			
x	0	0	0
$y = z$	0.481 (4)	0.483 (1)	0.5
Site occupancy	0.25	0.136 (9)	0.60 (5)
K3			
$x = y = z$		0.118 (3)	0.1547 (13)
Site occupancy		0.18 (2)	0.24 (1)
K4			
$x = y$		0.242 (6)	0.245 (4)
z		0.5	0.5
Site occupancy		0.04 (1)	0.08 (2)
K5			
$x = y$		0	
z		0.176 (7)	
Site occupancy		0.08 (2)	

TABLE 1b
Thermal Parameters for K_{12}-A and K_1/K_{12}-A

	K_{12}-A (295 K)	K_1/K_{12}-A (295 K)	K_1/K_{12}-A (4 K)
Si/Al			
B_{11}	0.90 (11)	1.1 (1)	0.4 (1)
B_{22}	0.65 (9)	1.3 (1)	0.9 (1)
B_{33}	0.36 (9)	0.8 (1)	0.0 (1)
B_{23}	0.45 (8)	−0.1 (1)	0.6 (1)
O1			
B_{11}	3.3 (2)	2.9 (2)	2.2 (2)
B_{22}	1.0 (1)	2.8 (2)	0.2 (1)
B_{33}	0.8 (1)	0.8 (1)	0.6 (1)
O2			
B_{11}	2.6 (2)	2.2 (1)	1.1 (1)
$B_{22} = B_{33}$	1.1 (1)	1.1 (1)	0.4 (1)
B_{23}	1.8 (1)	1.5 (1)	1.1 (1)
O3			
$B_{11} = B_{22}$	1.50 (6)	1.90 (6)	0.61 (5)
B_{33}	2.28 (10)	2.92 (12)	1.02 (8)
$B_{23} = B_{13}$	0.13 (5)	−0.04 (6)	0.03 (5)
B_{12}	1.37 (8)	1.08 (8)	0.48 (8)
K1			
$B_{11} = B_{22} = B_{33}$	3.7 (2)	2.5 (2)	0.6 (1)
$B_{23} = B_{13} = B_{12}$	1.8 (2)	1.7 (2)	0.3 (1)
K2			
B_{iso}	6.7 (13)	−0.4 (6)	1.3 (5)
K3			
B_{iso}		9.5 (22)	$=B$ for K1
K4			
B_{iso}		2	0.8 (11)
K5			
B_{iso}		2	

Note. R factors: K_{12}-A $R_{wP} = 2.1\%$, $R_E = 1.4\%$, $R_I = 8.3\%$;K_1/K_{12}-A (295 K), $R_{wP} = 3.3\%$, $R_E = 1.8\%$, $R_I = 7.1\%$;K_1/K_{12}-A (4 K), $R_{wP} = 3.9\%$, $R_E = 1.2\%$, $R_I = 11.5\%$.

$$R_{wP} = \left[\frac{\sum_i w_i |y_i(\text{obs}) - y_i(\text{calc})|^2}{\sum_i w_i y_i^2(\text{obs})}\right]^{1/2}, \quad R_E = \left[\frac{N - P + C}{\sum_i w_i y_i^2(\text{obs})}\right]^{1/2}, \quad R_I = \left[\frac{\sum_k |I_k(\text{obs}) - (1/c) I_k(\text{calc})|}{\sum_k I_k(\text{obs})}\right]$$

where N, P, and C are the number of observations, parameters, and constraints, respectively.

This site represents a conventional ion-exchange position previously reported for K_{12}-A (26). The distance between K3 and K1 across the 6-rings of the sodalite cage is too short (~2.5 Å) for both sites to be occupied simultaneously, even assuming complete potassium ionization. Since the sum of the refined occupancies of the two sites was slightly greater than 1, these were constrained in subsequent refinements. The large isotropic thermal parameter observed for this site indicates pronounced thermal motion of potassium in the sodalite cage. Indeed there was evidence for partial occupation of a further site (K5) in the sodalite cage coordinated to the 4-rings at (x, 0, 0) ($x \sim 0.17$). This implies that tumbling of potassium in the sodalite cage may occur, with these two sites representing minima. The indication of thermal motion within the sodalite cage at room temperature echoes a number of ESR studies which have made clear observations in zeolite A of the hyperfine splittings characteristic of Na_4^{3+} and K_3^{2+} centers only at reduced temperatures (8, 11). There was also a small amount of potassium (K4)

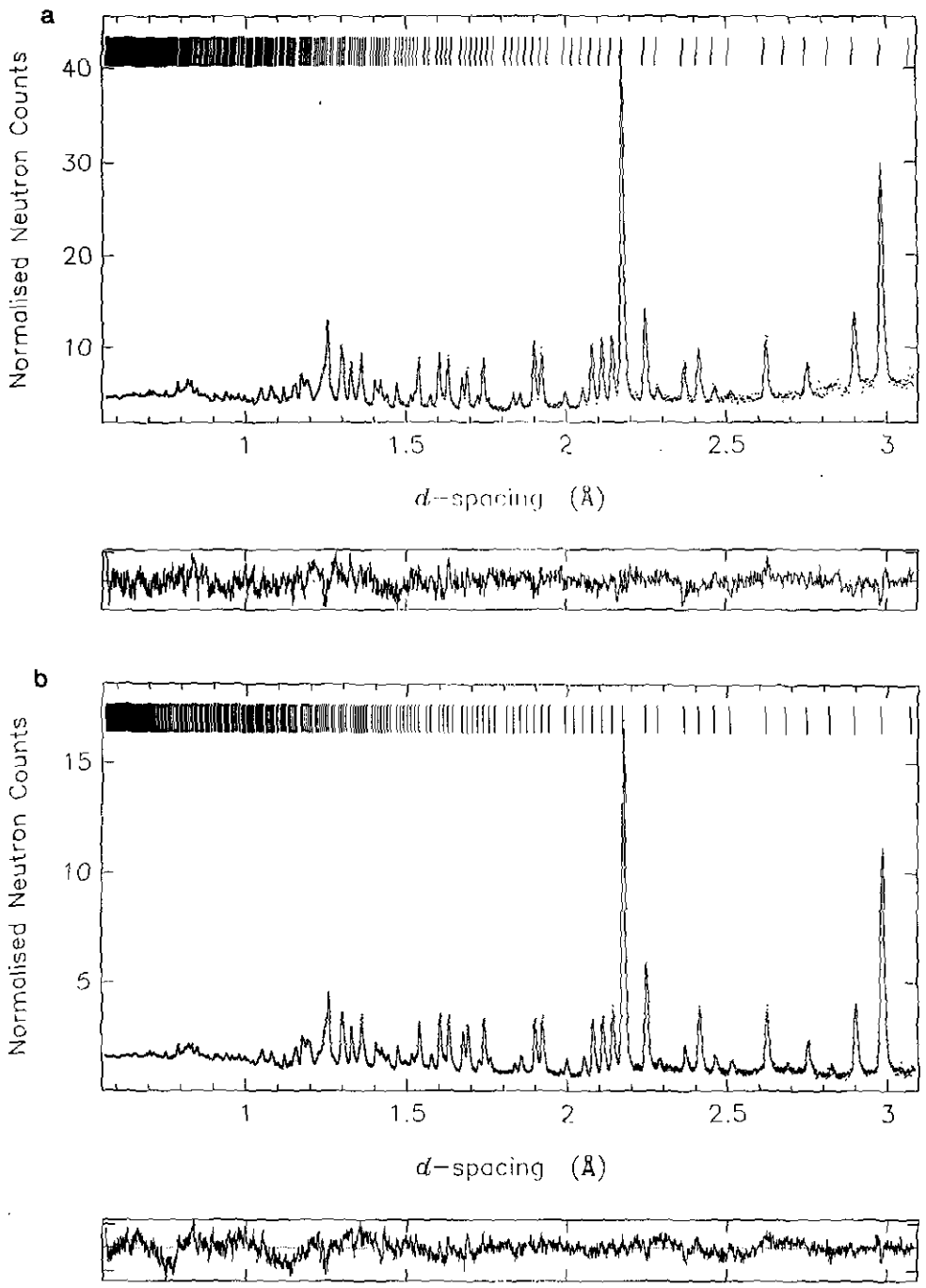

FIG. 1. Observed and calculated diffraction profiles for (a) K_{12}-A and (b) K_1/K_{12}-A at room temperature. The tick marks indicate allowed reflections in space group $Pm\bar{3}m$.

coordinated to the 4-rings in the α cages at $(x, x, 0.5)$ ($x \sim 0.24$). Final positional parameters are given in Tables 1a and 1b, and the profile fit is shown in Fig. 1b.

For the K_1/K_{12}-A data recorded at 4 K, slight changes were observed in the potassium distribution. Sites K3 and K4 were again occupied, but there was no evidence for potassium in the K5 site at $(x, 0, 0)$. Furthermore the K3 site was closer to the 6-rings ($x \sim 0.15$) and had much smaller thermal parameters (constrained in the final refinement). These observations indicate that tumbling had ceased, with the 6-ring site proving to be more stable. The refined occupancy of the K4 site underwent a slight increase on cooling. Since K1 and K3 sites cannot be occupied simultaneously, the increase in occupancy of

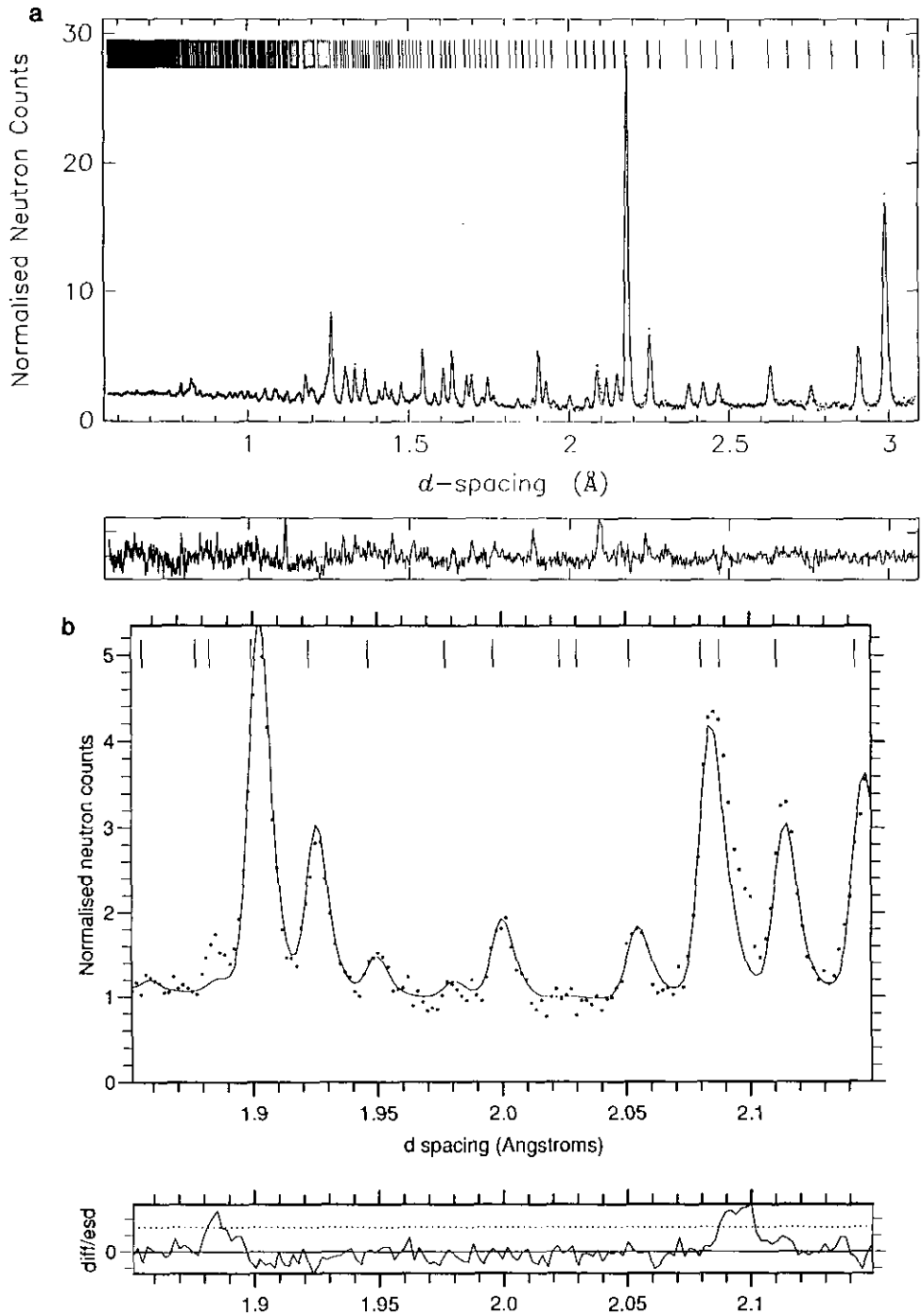

FIG. 2. Observed and calculated diffraction profiles for K_5/K_{12}-A. (a) Profile fit in space group $Pm\bar{3}m$ showing the presence of a number of superlattice reflections. (b) Profile fit in space group $Fm\bar{3}c$ (assuming Si/Al ordering) for a selected region of the diffraction pattern containing two superlattice peaks. Despite these reflections being allowed in this space group, they are not fitted. (c) Profile fit in space group $Fm\bar{3}m$ over the same region of the diffraction pattern as that shown in (b). The superlattice reflections are now very well fitted. (d) Profile fit in space group $Fm\bar{3}m$ for the full pattern.

K3 occasioned by the reduction in thermal motion, forces some of the potassium to move from the K1 position to the K4 position. Final positional parameters are shown in Tables 1a and 1b.

b. K_3/K_{12}-A and K_5/K_{12}-A

Refinement of the structure of K_5/K_{12}-A in space group $Pm\bar{3}m$, including potassium sites K1 and K2, gave a sat-

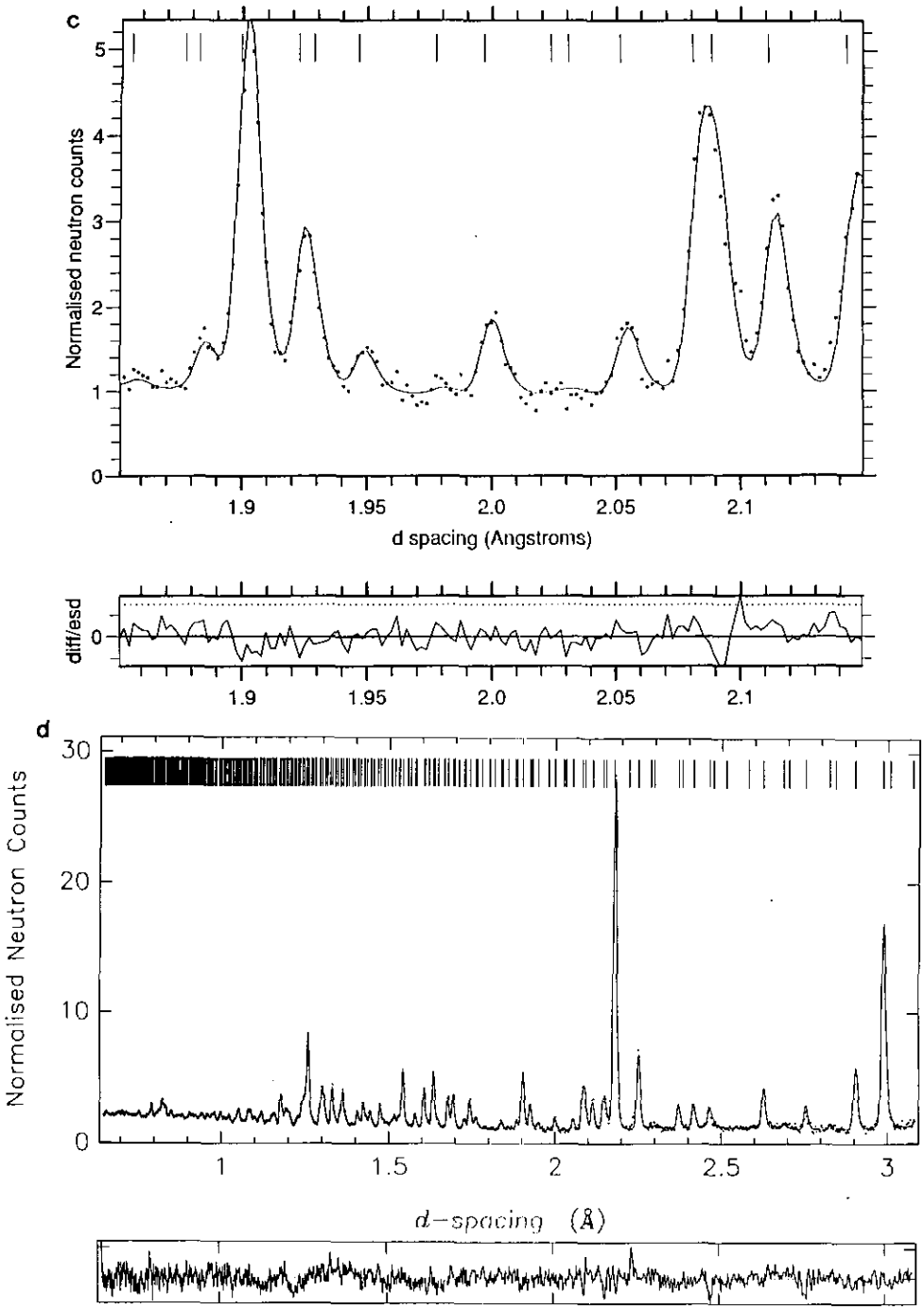

FIG. 2—Continued

isfactory fit to the data, confirming that the zeolite framework remained intact despite the very high level of metal loading. However, significant deviations between the observed and calculated intensities were apparent. Difference Fourier methods were used to locate further potassium sites: K3 in the sodalite cage at around (0.13, 0.13, 0.13) and K4 in the α cage at approximately (0.25, 0.25, 0.5). Inclusion of these two sites in the refinement resulted in a considerable improvement in the profile fit, as shown in Fig. 2a. While excellent R factors were obtained with this model, inspection of the difference between observed and calculated profiles reveals a number of apparent supercell relections. As indicated above, the supercell previously reported in zeolite A involves ordering of silicon and aluminium (space group $Fm\bar{3}c$) (28). Although adoption of this model gave an improved fit to

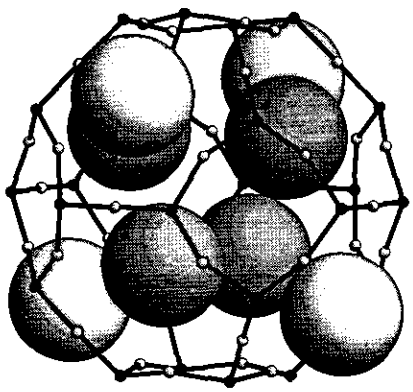

FIG. 3. The sodalite cage in K_5/K_{12}-A showing a tetrahedron of K3 ions inside the cage (dark circles) with faces capped by a tetrahedron of K1 ions outside the cage (pale circles).

the data, the prominent supercell reflections remained unfitted (Fig. 2b), implying that an alternative ordering mechanism was responsible.

A feature worthy of note is that the occupancies of sites K1, K3, and K4 all refined to values very close to 0.5. This is readily explained in the case of K1 and K3 since an impossibly short separation of 2.1 Å across the 6-rings of the sodalite cage prevents occupation of adjacent sites. Filling of a given K3 site thus forces potassium in the neighboring α cage to occupy the K4 site, which is presumably less stable than K1 since potassium can only achieve fourfold as opposed to sixfold coordination. This intrinsic topological constraint leads to cation ordering. The most energetically favorable arrangement for the four potassium ions per sodalite cage is a tetrahedron of K3, the faces of which can then be capped by a further tetrahedron of K1 as illustrated in Fig. 3. Each α cage contains on average 4 K1 and 6 K4, which cannot be accommodated without short K1–K4 interactions of 3.3 Å. A further ordering in which alternate α cages contain 8 K1 or 12 K4 removes the necessity for such short interatomic distances and can be accommodated in space group $Fm\bar{3}m$ (assuming that Si and Al are disordered over the tetrahedral sites). This ordered model gave a significantly improved refinement, successfully fitting all superlattice reflections as shown in Figs. 2c and 2d. Final crystallographic data are shown in Tables 2a and 2b.

Refinement of the structure of K_3/K_{12}-A proceeded along similar lines to that of the more heavily loaded K_5/K_{12}-A. The same potassium sites were occupied, and superlattice reflections were observed in $Pm\bar{3}m$ that were successfully fitted in $Fm\bar{3}m$. Refinement showed that the K1, K3, and K4 sites were no longer full, and the K3 and K4 exhibited reduced occupancy compared with K1. Partial filling of the K4 site leads to the remainder of the α cages in this sublattice containing sites equivalent to K1 (denoted by K1′). In addition some of the sites equivalent to K3 (denoted by K3′) were also found to be occupied. It is assumed that rather than a given sodalite cage containing more than four potassium ions, there are some sodalite cages in which the tetrahedron is inverted, resulting in depopulation of the K1 site. Similarly, it is believed that K1′ and K4 do not occur in the same α cage. The K4′ site was apparently not occupied. Final refined parameters are shown in Tables 2a and 2b and the profile fit is shown in Fig. 4. From these observations it is clear that while short range order is imposed at very low levels of added potassium by the short separation between K1 and K3, complete order is not reached until the zeolite is saturated with metal. K_3/K_{12}-A represents an intermediate between the two forms in which the structure contains sufficient potassium for a superlattice to form but is insufficient for perfect ordering.

One of the most important features of the refinements is that all four potassium sites observed in the potassium-loaded compounds have previously been found in the dehydrated zeolite itself (26, 27). The potassium sites may therefore be regarded as primarily ionic in character, and no distinction can be drawn between the potassium already present in the zeolite and that absorbed from the vapor phase. This represents convincing new evidence that the much postulated ionization of alkali metal atoms on entering a zeolite does in fact occur (6–16). It is the electrons released in this process, their properties and fate within the zeolite structure, and how they choose to interact with the complex three-dimensional array of cations presented to them that have up to now been the main source of interest in these compounds.

Seff and co-workers (17–21) have argued on purely crystallographic grounds for the existence of a diverse series of reduced cesium, rubidium, and potassium clusters mainly in zeolite A, and have also developed the concept of "cationic continua," where electrons are supposed to be delocalized throughout the zeolite crystals. In the absence of any measurements relating to electronic states in the compounds in question, however, the number and spatial extent of electrons associated with any particular group of cations must remain a matter for speculation, and it is unclear how the distinction between discrete clusters and extended "continua" is drawn. The dilemma is highlighted in a recent paper detailing the X-ray structure of zeolite A exposed to potassium vapor (21). The resulting compound contains 15 potassiums, 2 to 3 more than are necessary to balance the anionic charge of the zeolite framework, which are found in the same sites as those in this work. The authors present two possible scenarios as to the arrangement of ions within the α cages: ions in the K4 site can be reckoned either to be grouped in K_6^+ clusters or alternatively to form part of a complex "metallic continuum" extending throughout

TABLE 2a
Structural Parameters for K_3/K_{12}-A and K_5/K_{12}-A in Space Group $Fm\bar{3}m$

	K_3/K_{12}-A	K_5/K_{12}-A
Cell constant (Å)	24.6054 (1)	24.6324 (2)
Si/Al		
x	0.75	0.75
y	0.8433 (4)	0.8430 (2)
z	0.9385 (1)	0.9389 (1)
O1		
x	0	0
y	0.8725 (1)	0.8731 (2)
z	0.7451 (2)	0.7450 (2)
O2		
$x = y$	0.8922 (1)	0.8915 (1)
z	0.7542 (2)	0.7539 (3)
O3		
$x = y$	0.8073 (2)	0.8053 (2)
z	0.9327 (2)	0.9327 (2)
O4		
$x = y$	0.3056 (1)	0.3070 (2)
z	0.4270 (2)	0.4280 (3)
K1		
$x = y = z$	0.8664 (3)	0.8676 (4)
Site occupancy	0.83 (2)	1
K2		
$x = y$	0	0.0069 (10)
z	0.75	0.75
Site occupancy	0.62 (3)	0.140 (10)
K3		
$x = y = z$	0.3162 (2)	0.3177 (3)
Site occupancy	0.55 (3)	1
K4		
x	0.5	0.5
$y = z$	0.3718 (3)	0.3727 (3)
Site occupancy	0.71 (2)	1
K1′		
$x = y = z$	K1 x − 0.5	
Site occupancy	1 − K4 site	
K3′		
$x = y = z$	K3 x + 0.5	
Site occupancy	1 − K1 site	

TABLE 2b
Thermal Parameters for K_3/K_{12}-A and K_5/K_{12}-A

	K_2/K_{12}-A	K_5/K_{12}-A
Si/Al		
B_{11}	1.3 (1)	0.4 (1)
B_{22}	1.1 (1)	0.7 (1)
B_{33}	0.4 (1)	0.6 (1)
B_{23}	−0.4 (1)	0.1 (1)
B_{13}	−1.1 (1)	0.1 (2)
B_{12}	0.9 (1)	−0.1 (2)
O1		
B_{11}	1.3 (1)	1.8 (2)
B_{22}	1.2 (1)	1.0 (1)
B_{33}	2.1 (2)	1.5 (2)
B_{13}	0.1 (2)	0.9 (2)
O2		
$B_{11} = B_{22}$	1.2 (1)	0.8 (1)
B_{33}	1.2 (2)	1.5 (1)
$B_{23} = B_{13}$	−0.4 (1)	−0.5 (1)
B_{12}	1.4 (1)	1.0 (1)
O3		
$B_{11} = B_{22}$	2.9 (1)	2.3 (2)
B_{33}	1.9 (2)	1.1 (2)
$B_{23} = B_{13}$	0.0 (1)	−0.3 (1)
B_{12}	0.5 (2)	−0.1 (3)
O4		
$B_{11} = B_{22}$	1.0 (1)	1.3 (1)
B_{33}	0.9 (1)	1.8 (2)
$B_{23} = B_{13}$	−0.4 (1)	0.4 (1)
B_{12}	1.1 (1)	0.1 (2)
K1 = K1′		
$B_{11} = B_{22} = B_{33}$	3.2 (3)	2.1 (3)
$B_{23} = B_{13} = B_{12}$	0.5 (2)	0.5 (3)
K2		
B_{iso}	2.9 (5)	0.0 (7)
K3 = K3′		
$B_{11} = B_{22} = B_{33}$	0.4 (2)	2.0 (2)
$B_{23} = B_{13} = B_{12}$	1.6 (2)	1.4 (3)
K4		
B_{11}	1.6 (5)	2.3 (6)
$B_{22} = B_{33}$	1.4 (3)	2.6 (4)
B_{23}	0.9 (3)	−0.4 (4)

Note. R factors: K_3/K_{12}-A R_{wP} = 2.9%, R_E = 2.3%, R_I = 6.2%; K_5/K_{12}-A, R_{wP} = 4.2%, R_E = 2.5%, R_I = 6.6%.

the zeolite structure. This ambiguity in cation arrangements, which arises from the need to interpret fractional occupancies, has now been removed by the detection of a superlattice in K_5/K_{12}-A, but the distribution of electrons amongst the ions is as tricky as ever to pin down.

In a range of sodium and potassium zeolites, ESR studies have shown that "excess" electrons released through the ionization of alkali metal atoms entering the zeolite may be found trapped in paramagnetic centers of the form $M_n^{(n-1)+}$, consisting of an electron delocalized over a

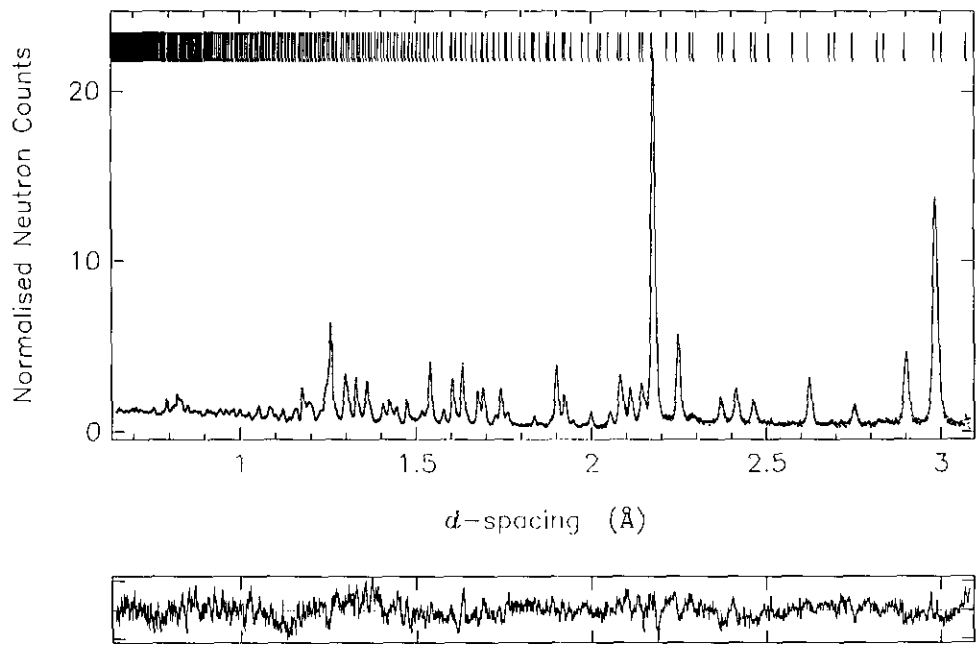

FIG. 4. Observed and calculated diffraction profiles for K_5/K_{12}-A in space group $Fm\bar{3}m$.

well-defined number of cations (6–14). Recently, the first signs of more extensive delocalization have also been noted (11, 14, 15). The room temperature ESR spectra of the three potassium-loaded compounds are shown in Fig. 5. It is important to make the point that no hyperfine structure was observed in the spectrum of these samples, even at 77 K. It follows that even though we can point to the refined structure of K_5/K_{12}-A as the first *unambiguous* demonstration of the presence of a tetrahedron of cations within the sodalite cage (Fig. 4), we must be careful in identifying this structural feature as a K_4^{n+} cluster. The absence of metal hyperfine splitting is not consistent with the presence of isolated unpaired electron spins (11).

The concept of bond valence sums (BVS) devised by Brown has been widely applied to estimate valences in inorganic solids, most recently in the field of high-temperature superconductivity (29, 30). BVS for potassium in K_5/K_{12}-A have been calculated using the formula of Brown and Altermatt (30). While these should be treated with caution in view of the imperfect coordination obtained by potassium in lining the zeolite cavities, K1 and K3 are directly comparable since both are coordinated to the 6-rings of the sodalite cage. Interestingly, whereas K1 behaves as K^+, the value for the K3 tetrahedron within the sodalite cage is close to the 0.75 value expected for K_4^{3+}. Although the absolute values may be misleading, the K3 ions do appear to be electron rich compared with K1. One explanation for this might be that the sodalite cages do in fact contain K_4^{3+} centers, but that the chararacteristic hyperfine splitting pattern is absent ow-

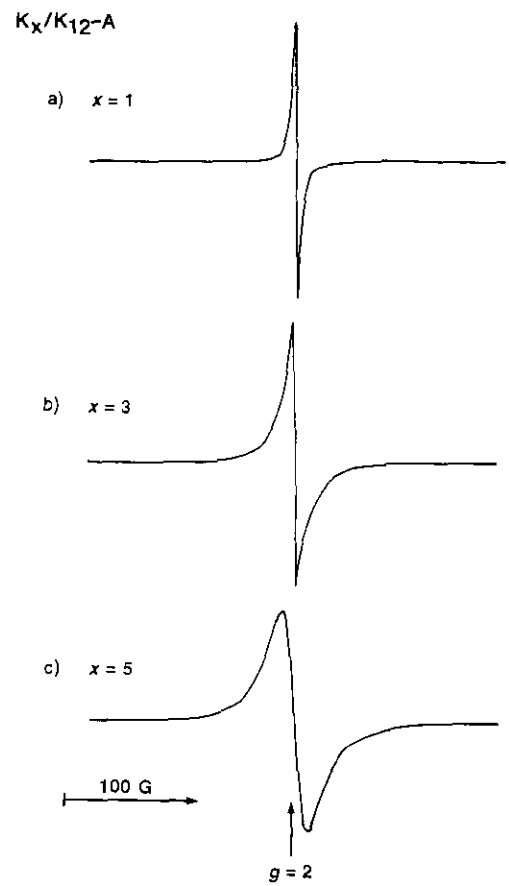

FIG. 5. Room temperature ESR spectra for (a) K_1/K_{12}-A, (b) K_3/K_{12}-A, and (c) K_5/K_{12}-A.

ing to interactions between centers in neighboring cages, as is reported to occur in sodium zeolites (11). Alternatively, the number may reflect the K3 cations' "share" of electrons which are not confined to the sodalite cage but exhibit more extensive delocalization. In this respect it is important to mention that although K_1/K_{12}-A contains exactly the right number of excess electrons to provide for the formation of a K_4^{3+} (or possibly K_3^{2+}) center in each sodalite cage, the actual occupancy of the K3 site indicates that this does not happen. Even at modest metal loadings, it would appear that substantial electron density resides in the α cages.

The possibility of the delocalization of excess electrons throughout the zeolite structure draws attention to a unique feature of compounds such as K_5/K_{12}-A: a ration of five such electrons per 17 potassium ions would leave this hypothetical metal notionally electron-deficient with less than 0.3 itinerant electrons per cation. As a consequence of potassium ordering, moreover, the distribution of potassium in both K_3/K_{12}-A and K_5/K_{12}-A is far from homogeneous, despite the apparent saturation of the latter with metal. The α cages containing 8 K1 ions retain the structure of the parent zeolite, while those containing up to 12 K4 are much more densely packed (Fig. 6). Although a low bond valence sum for K4 (0.5) may in part be ascribed to its lower coordination number, these ions also appear electron-rich compared with K1. Apparently both electronic and structural segregation has occurred in K_5/K_{12}-A, with half the α cages remaining as pristine pockets of dehydrated zeolite, and with the excess electrons confined to a cationic network located in the sodalite cages and the more densely occupied α cages. Both the ESR g value and the potassium–potassium nearest neighbor distances in the denser region of the structure are comparable to those observed in the bulk metal (31, 32). In K_5/K_{12}-A these potassium–potassium distances fall in the range 4.238Å(13) to 4.884(11) Å, compared with a value of 4.54 Å for potassium metal (32). The potassium–potassium distances in K_5/K_{12}-A are given in Table 3.

TABLE 3
Potassium–Potassium Bond Lengths in K_5/K_{12}-A

K1–K1	5.794(9)	×3				
K1–K2	5.245(13)	×3	5.452(13)	×2	5.652(14)	×1
K1–K3	4.884(11)	×3				
K2–K4	4.238(13)	×2	4.482(13)	×2		
K3–K3	4.719(8)	×3				
K3–K4	4.880(8)	×3				
K4–K4	4.436(5)	×4				

As a result of this work we can build up a comprehensive picture of the progressive filling of the structure of zeolite A with potassium. At low loadings occupation of the K3 site in the sodalite cages begins. It is tempting to speculate that this occurs as a result of the formation of K_3^{2+} or K_4^{3+}, although there is no direct ESR evidence for this in the samples studied. Since this site and K1 cannot be occupied simultaneously the additional potassium is accommodated in the K4 sites. In lightly loaded material at room temperature the potassium in the sodalite cages is quite mobile, the motion being frozen out at low temperatures. This motion may explain the nonobservance of the K_3^{2+} at room temperature—although K_3^{2+} is not observed in K_1/K_{12}-A it is reasonable to infer that similar tumbling would occur at lower loadings. As more potassium is introduced to the structure the constraints imposed by the closeness of K1 and K3 (and also K1 and K4) become more important. These constraints appear to prevent potassium tumbling in the sodalite cage and result in superlattice formation and long-range potassium order. This ordering is incomplete until an apparently limiting composition is reached.

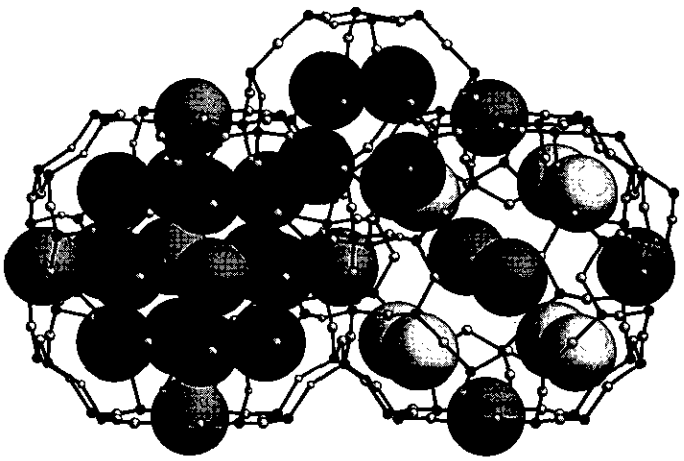

FIG. 6. Fragment of the structure of K_5/K_{12}-A showing neighboring α cages and a sodalite cage. The much less open structure of the left-hand cage containing K4 is readily apparent. The different ionic sites have different shadings.

ACKNOWLEDGMENTS

We thank the SERC for support and provision of neutron beam facilities. The structure diagrams were drawn using ATOMS by Shape Software. P.A.A. is a Royal Society Research Fellow. It is a great pleasure and honor to be part of this volume celebrating the marvelous science of C.N.R. Rao on his 60th birthday.

REFERENCES

1. R. M. Barrer, "Hydrothermal Chemistry of Zeolites." Academic Press, London, 1982.
2. G. A. Ozin, A. Kuperman, and A. Stein, *Angew. Chem. Int. Ed. Engl.* **28**, 359 (1989).
3. G. D. Stucky and J. E. MacDougall, *Science* **247**, 669 (1990).
4. J. A. Rabo, C. L. Angell, P. H. Kasai, and V. Schomaker, *Discuss. Faraday Soc.* **41**, 328 (1966).

5. P. H. Kasai, *J. Chem. Phys.* **43,** 3322 (1965).
6. P. P. Edwards, M. R. Harrison, J. Klinowski, S. Ramdas, J. M. Thomas, D. C. Johnson, and C. J. Page, *J. Chem. Soc. Chem. Commun.*, 982 (1984).
7. M. R. Harrison, P. P. Edwards, J. Klinowski, J. M. Thomas, D. C. Johnson, and C. J. Page, *J. Solid State Chem.* **54,** 330 (1984).
8. P. A. Anderson, R. J. Singer, and P. P. Edwards, *J. Chem. Soc. Chem. Commun.*, 914 (1991).
9. P. A. Anderson and P. P. Edwards, *J. Chem. Soc. Chem. Commun.* 915 (1991).
10. P. A. Anderson, D. Barr, and P. P. Edwards, *Angew, Chem.* **103,** 1511 (1991); *Angew. Chem. Int. Ed. Engl.* **30,** 1501 (1991).
11. P. A. Anderson and P. P. Edwards, *J. Am. Chem. Soc.* **114,** 10608 (1992).
12. G. Schäfer, W. W. Warren, P. A. Anderson, and P. P. Edwards, *J. Non-Cryst. Solids* **156–158,** 803 (1993).
13. P. Sen, C. N. R. Rao, and J. M. Thomas. *J. Mol. Struct.* **146,** 171 (1986).
14. P. P. Edwards, P. A. Anderson, A. R. Armstrong, M. Slaski, and L. J. Woodall, *Chem. Soc. Rev.* **22,** 305 (1993).
15. P. A. Anderson, A. R. Armstrong, and P. P. Edwards, *Angew. Chem.* **106,** 669 (1994); *Angew. Chem. Int. Ed. Engl.* **33,** 641 (1994).
16. A. R. Armstrong, P. A. Anderson, and P. P. Edwards, *J. Chem. Soc. Chem. Commun.* 473 (1994).
17. T. Sun, K. Seff, N. H. Heo, and V. P. Petranovskii, *Science* **259** 495 (1993).
18. T. Sun and K. Seff, *J. Phys. Chem.* **97,** 5213 (1993).
19. S. H. Song, U. S. Kim, Y. Kim, and K. Seff, *J. Phys. Chem.* **96,** 10937 (1992).
20. N. H. Heo and K. Seff, *J. Am. Chem. Soc.* **109,** 7986 (1987).
21. T. Sun and K. Seff, *J. Phys. Chem.* **97,** 10757 (1993).
22. H. S. Sherry, *J. Phys. Chem.* **70,** 1158 (1966).
23. J. C. Matthewman, P. Thompson, and P. J. Brown, *J. Appl. Crystallogr.* **15,** 167 (1982).
24. P. J. Brown and J. C. Matthewman, Rutherford Appleton Laboratory Report, RAL-87-010, 1987.
25. V. F. Sears, *Neutron News* **3**(3), 26 (1992).
26. J. J. Pluth and J. V. Smith, *J. Phys. Chem.* **83,** 741 (1979).
27. P. C. W. Leung, K. B. Kunz, K. Seff, and I. E. Maxwell, *J. Phys. Chem.* **79,** 2157.
28. V. Gramlich and W. M. Meier, *Z. Kristallogr.* **133,** 134 (1971).
29. I. D. Brown, *Chem. Soc. Rev.* **7,** 359 (1978).
30. I. D. Brown and D. Altermatt, *Acta Crystallogr. Sect.* B **41,** 244 (1985).
31. R. C. McMillan, *J. Phys. Chem. Solids* **25,** 773 (1964).
32. N. N. Greenwood and A. Earnshaw, "Chemistry of the Elements," Pergamon Press, Elsford, NY.